



A Series of Isorecticular, Highly Stable, Porous Zirconium Oxide Based Metal–Organic Frameworks**

V. Guillerm, F. Ragon, M. Dan-Hardi, T. Devic, M. Vishnuvarthan, B. Campo, A. Vimont, G. Clet, Q. Yang, G. Maurin, G. Férey, A. Vittadini, S. Gross, and Christian Serre*

Metal–organic frameworks (MOFs) are hybrid porous solids that have recently attracted great interest for potential applications including gas separation/storage, catalysis, sensors, inclusion, and drug delivery.^[1–5] However, there are still concerns about the chemical and mechanical stabilities of this class of materials. The poor hydrothermal stability of most MOFs is clearly a limitation for their use in real separation processes.^[6] MOFs with enhanced stability are also required for liquid-phase catalysis applications, such as the production of hydrogen from water splitting.^[7] Willis et al. have performed a systematic study showing that for a given linker, increasing the charge of the metal usually leads to an enhancement of the hydrothermal stability of the resulting MOF.^[6a] To date, porous MOFs based on polycarboxylate and tetravalent metals are still scarce with only a few such solids being accessible to nitrogen molecules.^[8–10] Among them, the titanium(IV) terephthalate MIL-125 (MIL stands for Materials from Institut Lavoisier)^[10] and the zirconium terephthalate UiO-66(Zr) (UiO for University of Oslo),^[9] which both have

a 3D microporous cubic pore system, are of interest because of their relatively high stability combined with large accessible pore volumes. For instance, UiO-66(Zr) is stable up to 450°C under air and remains unaltered upon water adsorption/desorption cycles by switching reversibly between dehydroxylated and hydroxylated versions,^[9,11] and has an exceptional stability under mechanical stimulus.^[9] Recently, a series of derivatives of the UiO structure has been obtained using either functionalized or extended dicarboxylate linkers.^[12] Others have reported the use of inhibitors to control the crystallization process of these UiOs^[13] while some of us have established that by using pre-defined oxo clusters as secondary building units (SBU), UiO-66(Zr) analogues can be prepared at low temperature.^[14] These recent results show that the chemistry of tetravalent-metal-based carboxylate MOFs is “accessible”, although the synthesis conditions and the structure determination are challenges related to the very high reactivity of M⁴⁺ ions in the presence of polar solvents.

We report herein the solvothermal synthesis of new porous zirconium dicarboxylate MOFs based on the reactions of ZrCl₄ with 1,4-H₂BDC (1,4-benzenedicarboxylic acid), 2,6-H₂NDC (2,6-naphthalenedicarboxylic acid), 4,4'-H₂BPDC (4,4'-biphenyldicarboxylic acid), and H₂Cl₂ABDC (3,3'-dichloro-4,4'-azobenzenedicarboxylic acid). A whole new series of porous zirconium dicarboxylate solids, denoted MIL-140A to MIL-140D, with a general formula [ZrO(O₂C-R-CO₂)] (R = C₆H₄ (MIL-140A), C₁₀H₆ (B), C₁₂H₈ (C), C₁₂N₂H₆Cl₂ (D)) has been isolated and characterized, and their properties compared with those of the polymorphs UiO-66 and its upper analogues (that is, solids of the same structure type but with longer organic spacers). The crystal structures have been either solved using X-ray powder diffraction (XRPD) data or through a computational assisted strategy based on density functional theory (DFT) geometry optimizations. The MIL-140 solids crystallize in the space group (SG) C2/c (No. 15) (MIL-140A and C) or Cc (No. 9) (MIL-140B and D; Supporting Information, Table S3). These solids all have the same *c* parameter (ca. 7.8 Å), consistent with the inorganic subunit of complex zirconium oxide chains, oriented along the *c* axis (Figure 1), connected to six other chains through the dicarboxylate linkers. This delimits triangular channels along the *c* axis. The zirconium atoms exhibit a seven coordination mode with three μ₃-O oxygen atoms and four oxygen atoms from the dicarboxylate groups. Inorganic chains can be considered either as resulting from the linkage of two parallel corner-sharing chains or chains of edge-sharing dimers of zirconium polyhedra. These chains could be considered as being repeating tetramers of Zr polyhedra, such as those observed in monoclinic ZrO₂^[15] or in the mixed

[*] Dr. V. Guillerm,^[+] F. Ragon,^[+] Dr. M. Dan-Hardi, Dr. T. Devic, Prof. G. Férey, Dr. C. Serre
Institut Lavoisier, UMR 8180 CNRS Université de Versailles St Quentin en Yvelines
45 avenue des Etats-Unis, 78035 Versailles (France)
E-mail: serre@chimie.uvsq.fr
Dr. M. Vishnuvarthan, Dr. B. Campo, Dr. A. Vimont, Dr. G. Clet
Laboratoire Catalyse et Spectrochimie, Ensicaen, Université de Caen, CNRS
6 Bd du Maréchal Juin, 14050 Caen (France)
Prof. Q. Yang, Prof. G. Maurin
Institut Charles Gerhardt, UMR CNRS 5253, ENSCM - CNRS - UMI - UMII, Université Montpellier 2
34095 Montpellier cedex 05 (France)
Prof. Q. Yang
State Key Laboratory of Organic-Inorganic Composites, Beijing University of Chemical Technology
Beijing 100029 (China)
Dr. A. Vittadini, Dr. S. Gross
ISTM-CNR, Dipartimento di Scienze Chimiche and INSTM, UdR Padova, Università degli Studi di Padova
via Marzolo 1, 35131 Padova (Italy)

[+] These authors contributed equally to this work.

[**] This work has been performed within the frame of the ANR “NOMAC” (ANR-06-CO₂-008) and the Macademia European Community's Seventh Framework Program (FP7/2007-2013) under grant agreement n° 228862. Farid Nouar is thanked for this help with TOPOS and G. Le Bars for some IR measurements. Diamond Synchrotron Beamline I11 for part of the XRPD data collection.

Supporting information for this article is available on the WWW under <http://dx.doi.org/10.1002/anie.201204806>.

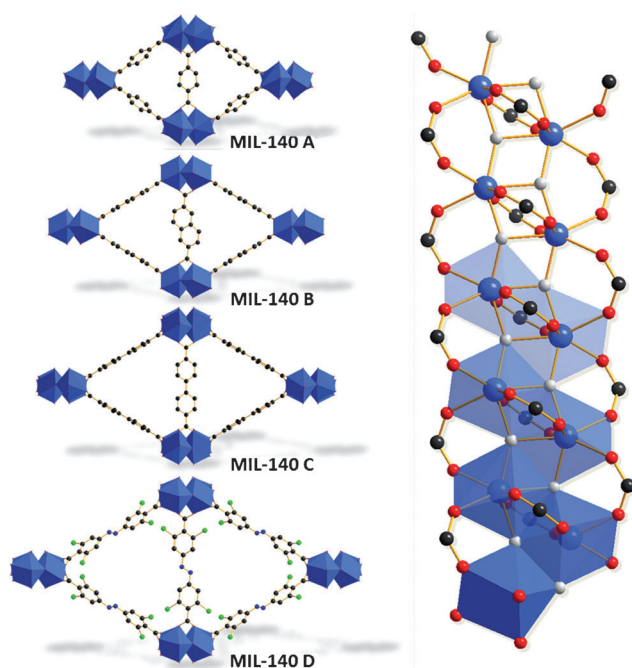


Figure 1. Left: view of the crystal structure for the series of MIL-140(Zr) solids along the *c* axis. Right: view of the inorganic subunit of MIL-140. Zr atoms or polyhedra blue, C black, and Cl green. Oxygen atoms from the linker are red and oxo groups are gray. Cl atoms in MIL-140D are disordered with a 50% site occupancy.

metal (Zr-Ti) methacrylate oxo cluster containing seven and eight coordinated zirconium cations.^[16] The structure of MIL-140 exhibits the uninodal 6c β Sn? (Figure S17).^[17] Each atom from the dense inorganic β Sn structure is connected to six other nets making a distorted octahedron.^[18] The Sn metal atom is replaced in this case by an infinite chain of Zr oxide. Such a β Sn topology is not common in MOFs.^[19]

The so-obtained connectivity within an infinite SBU has, to our knowledge, never been observed, even considering the existence of MOFs based on edge-sharing polyhedra, such as the iron or aluminum tetracarboxylate MOFs.^[20] The MIL-140 structure can also be compared with that of the porous scandium MOF denoted ScBDC solid^[21] or the vanadium terephthalate MIL-47 in which lozenge shape 1D pores are present but each inorganic chain is related to only four other chains.^[22] The higher chain connectivity encountered in MIL-140 originates from the higher coordination number of zirconium (7) compared to vanadium (6) as well as from the presence of a complex “double chain” inorganic SBU instead of a simple chain of corner-sharing octahedra in MIL-47. Thus, additional linkages between the inorganic subunits perpendicular to the chains, “transforms” the lozenge-shaped tunnels from MIL-47 into triangular ones in MIL-140.

Unlike the UiO series (formulated as $[\text{Zr}_6\text{O}_4(\text{OH})_4(\text{O}_2\text{C-R-CO}_2)_6]$,^[9,11,23] no structural hydroxy groups but only minor amounts of coordinated water were identified by IR spectroscopy on the MIL-140s (Figures S2–S4). This composition was reflected by the lack of any Brønsted acidity of these solids. Conversely Lewis acid sites were detected by the presence of an adsorption band characteristic of coordinated

CD_3CN species ($\nu(\text{CN})$ at ca. 2300 cm^{-1}). This band is at the same position for all the MIL-140 solids, which implies a similar acid strength. However, the intensity of the band, hence the amount of Lewis acid sites detected by CD_3CN , varies from one solid to the other (Figure 2). While compa-

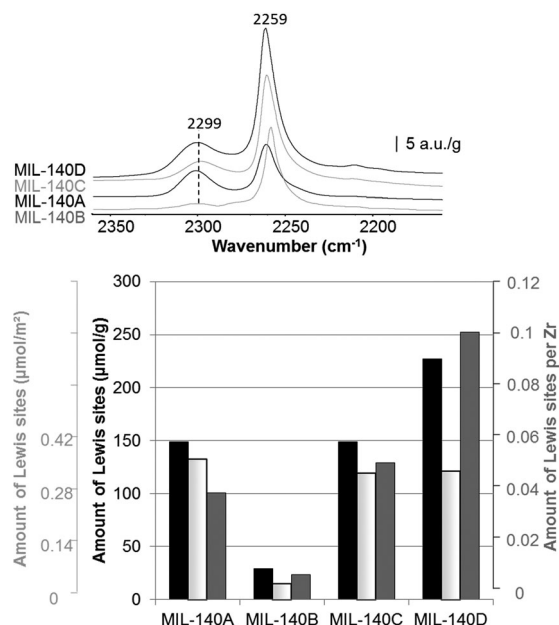


Figure 2. Acidity of the MIL-140s determined by CD_3CN adsorption. Top: FTIR spectra. Bottom: Density of Lewis acid sites, based on the mass of the solid (black bars; left scale), to its BET surface area (light gray bars; outer left scale), or to the number of Zr atoms (dark gray bars; right scale).

table for MIL-140A and C, the concentration of Lewis acid sites is highest for MIL-140D, however MIL-140A, C, and D have similar values when expressed in amount of sites per m^2 of surface area. Noteworthy, the amount of Lewis sites on MIL-140D represents one tenth of the Zr atoms which compares well with the values obtained for UiO-66.^[11] The presence of Lewis acid sites could be tentatively attributed to acidic sites on the external surface. However, this is unlikely, as pyridine, which is not expected to enter the pores of MIL-140A, should be adsorbed just as well on the external surface, which is not the case. Only a very small amount of sites were detected for MIL-140B, which was further confirmed by both pyridine and CO adsorption at 77 K. Nevertheless, the low amount of coordinately unsaturated sites (less than 10% of the Zr atoms) precludes their identification by PXRD. These Lewis acid sites could originate from 1) the dehydration of coordinated species, such as for UiO-66, 2) the presence of defects^[12a,24], or 3) a local change in the coordination mode of the Zr atoms upon adsorption of species, as observed for porous Ln carboxylate MOFs.^[25]

Further, as the refined crystal structures do not indicate the presence of any significant hydrogen-bond acceptor or donor site, except for MIL-140D, it could be expected that MIL-140s are hydrophobic. Indeed, to reach a perfectly activated porous solid, the costly complete removal of residual water from hydrophilic MOFs must be considered.

Thermogravimetric analysis (TGA) and IR spectroscopy were therefore used to qualitatively assess the hydrophobic character of these solids. TGA measurements have shown that the samples exhibit almost no loss of free water (Supporting Information Figure S18).

Optical water vapor adsorption isotherms have been collected (Figure S29) and show that these solids can be considered as being more hydrophobic than the UiO-66 counterpart which is fully loaded with water at intermediate humidity rate ($P/P_0 = 0.5$):^[11] Only a little adsorption occurs at low pressure, particularly for the smaller pore size MIL-140A and B solids, probably corresponding to coordination to the metal sites; at higher pressure, a filling of the pores starts, as typically observed for some activated carbons or siliceous zeolites,^[26] even if no sharp adsorption step is observed. Albeit not as hydrophobic as fluorinated MOFs,^[11] the MIL-140s can be considered as rare examples of slightly hydrophobic porous solids that have a significant amount of Lewis acid sites.

As a consequence of the 1D pore system, the pore size and volume of the MIL-140s are smaller than for the UiO series, for which experimental and/or theoretical specific surface areas^[27] range from 1000 to 3500 m² g⁻¹ (Figure S26, S27). The pore size distributions (PSD) of the MIL-140A–D structures were estimated by the method reported by Gelb and Gubbins.^[28] The pore sizes are roughly 3.2, 4.0, 5.7 and 6.3 Å respectively (Figure S20). The experimental BET surface areas were further determined at 415(10), 460(10), 670(20) and 701(20) m² g⁻¹, respectively for the activated MIL-140A–D samples. Values for MIL-140C and D are lower than the theoretical BET surface areas from their simulated adsorption isotherms of N₂ at 77 K, obtained by Grand Canonical Monte Carlo simulations (841 and 875 m² g⁻¹, respectively, Figures S24 and S25).^[27] Such a deviation can be explained by the presence of residual Zr oxide as evidenced by TGA and elemental analysis (Figure S19, Table S4). Further, while the theoretical BET values are similar to the accessible surface areas for the MIL-140C and D, a situation that validates the use of the geometric method for these solids with medium pore sizes, the situation drastically differs for the small pore MIL-140A and B structures. Their theoretical BET surface areas deduced from experimental isotherms (360 and 429 m² g⁻¹, respectively) are much more reliable than the accessible surface areas (0 and 149 m² g⁻¹) and fit well the experimental value. This result can be related to previous studies^[29] which have emphasized that the side pockets of the mordenite type zeolite cannot be probed using the geometric method. Thus, the geometric approach is not suitable for adsorbents with a pore size comparable to those of N₂. The consideration of the pore volume is an alternative way to circumvent such limitations and further characterize the ultra-small pore sizes structures. The thermodynamic pore volumes calculated (Table S9) lead to values of 0.10, 0.21, 0.35, 0.36 cm³ g⁻¹ for MIL-140A, B, C, and D (exp: 0.18, 0.18, 0.27, 0.29 cm³ g⁻¹, respectively).

To further assess the thermal stability of the two sets of porous Zr MOFs, that is, the UiO-66 and MIL-140 series, combined TGA and X-ray powder diffractometry analysis were carried out (Figures S18 and S19). It appears that MIL-

140s are highly stable with a slightly higher thermal stability, of around 500°C under air, against 450°C for the UiOs. As a further step, the hydrothermal and mechanical stability of the MIL-140 series were explored and compared to the corresponding UiO-66 analogues.

The industrial use of an adsorbent requires both moisture (or hydrothermal) and mechanical stability to avoid structural distortion or framework collapse under hydrostatic compression during the shaping steps.^[30,31] First, it appears, based on XRPD analysis, that MIL-140 compounds are hydrothermally stable, that is, after an overnight dispersion in deionized water at 100°C (Figure 3), no loss of crystallinity occurs, even for the upper analogues. The UiO-66(Zr) solid also retains its crystallinity upon the same treatment, but this is not the case for the upper UiO analogues, for which only poorly crystalline samples are recovered (Figure S28).

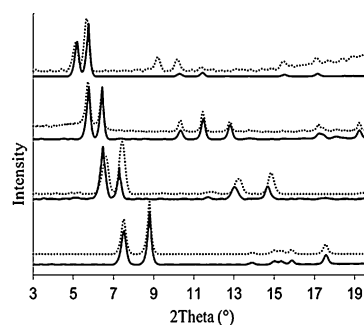


Figure 3. XRPD of MIL-140A, B, C, and D (from bottom to top) ($\lambda_{Cu} = 1.5406$ Å). Before water treatment (solid line), after hydrothermal treatment (100°C, 15 h; dotted line).

Interestingly, no peaks from the recrystallized dicarboxylate linkers are observed after the hydrothermal treatment. Considering the poor solubility of these linkers in water and the position of the remaining diffraction peaks of the sample after hydrothermal treatment, close to the main peaks of the initial phase, this data suggest a loss of long range order only. Thus, either the hydrothermal treatment leads to a partial degradation of the starting UiO material or to the formation of poorly crystalline MIL-140 solids through a dissolution recrystallization process. To assess this hypothesis, the reactivity of the Cl₂H₂ABDC/Zr⁴⁺ pair in DMF was explored at various temperatures (150–200°C; Figure S1). While UiO solid is formed at low temperature (150–160°C), a further increase of the temperature leads first to a dissolution of the phase and the recrystallization of MIL-140D at 180°C. Similarly, UiO-66 and MIL-140A are obtained in DMF at 150°C or 220°C, all other conditions (reactants, time, etc.) being kept identical. Thus, it can be estimated that UiOs and their polymorph MIL-140s are the kinetic or thermodynamic phases, respectively. To our knowledge, this is the first time that a series of isorecticular extended solids exhibits a hydrothermal stability. The higher hydrothermal stability of the MIL-140s, compared to the UiOs, could be due to the inorganic building units, that is, infinite Zr oxide chains versus isolated Zr₆O₄(OH)₄ oxoclusters for the UiO structures,

which have an inherently low hydrolytic stability undergoing hydrolysis of the Zr–O bonds.

However, first systematic studies discussing the criteria for the hydrothermal stability of MOFs pointed out that such a stability could be related to the capability of exchanging an oxygen (or nitrogen) atom from the coordination sphere of the metal by an oxygen atom from a water molecule.^[6]

Our calculations show that the overall framework energy increases with the length of the linker (Supporting Information). There is thus no difference in water stability upon changing the organic spacer within a series of isoreticular MOFs. As shown for UiO-66 and the lability of the ligands in solution,^[32] this means that other parameters (e.g., entropy) have to be considered for a realistic explanation of the hydrothermal stability of MOFs.

Finally, the effect of pressure has been studied on the UiOs and MIL-140s. The solids were subjected to an increasing uniaxial compression using a IR press and examined by XRPD (Figure 4 and Figure S30), allowing their overall crystallinity to be checked (related to the width of the Bragg peaks, Supporting Information). Again, as shown herein for UiO-66 and MIL-140C, which both have a crystal density close to 1.2 g cm⁻³ (Figure 4), MIL-140 solids on the

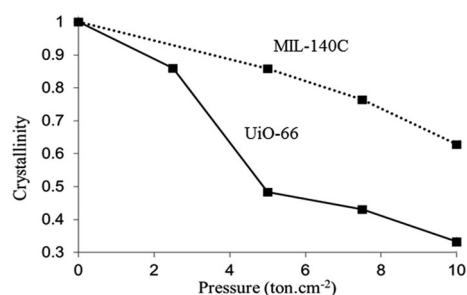


Figure 4. Evolution of the crystallinity of MIL-140C and UiO-66 after exposure to an increasing uniaxial mechanical pressure.

whole have a better stability than their UiO counterparts over this pressure range. Noteworthy, the longer the linker the lower the mechanical stability. According to Cheetham and Tan^[33] this observation is related to the framework density, which varies for the MIL-140s from 1.74 down to 1.23 g cm⁻³ while with the same spacer, the density of the corresponding UiOs is much lower, that is, from 1.2 down to 0.70 g cm⁻³. Thus, the higher mechanical stability of the MIL-140 series might only be a matter of density. Recently, the relative isostatic stability of a series of ZIFs type compounds based on zinc, lithium, or boron has been analyzed.^[34] If a relationship between the density of the porous solid and its Young modulus exists, the importance of the flexibility and stiffness of the inorganic SBU has been highlighted.

For instance, on replacing Zn–Im–Zn by Li–Im–B within the same structure (Im: imidazolate), the higher degree of flexibility around Li or B results in lower stability. Considering MIL-140C and UiO-66, which have similar density and pore volume, the higher mechanical stability of MIL-140C might thus arise from a less-flexible character of the infinite double chain of zirconium oxide compared to the Zr₆

oxoclusters. In addition, the presence of π stacking for 50 % of the aromatic linkers in MIL-140 solids also brings short-range dispersive interactions which might enhance the stability of the framework.

To assess this hypothesis, dispersion-corrected DFT calculations on neutral terephthalic acid (BDC) molecules (Figure S39), allowed us to estimate that the π -stacking energy in MIL-140A is 0.25 eV unit⁻¹ (i.e. 1 eV cell⁻¹) and that the binding energy of a BDC π dimer with the same geometry is 0.23 eV. Notably, these values are only slightly higher than the 0.098 eV value computed with the same approach for benzene dimerization.^[35] The stacking interaction in MIL-140A is comparable to that present in BDC crystals, which favors an increased mechanical stability of MIL-140.

In summary, we report for the first time a series of porous Zr oxide dicarboxylate MOFs that combines a relatively pronounced hydrophobic character and Lewis acidity, a high hydrothermal and a good mechanical stability. This paves the way for their use for applications, such as catalysis, adsorption, or separation.

Experimental Section

XRPD data were collected using a laboratory Bruker D5000 source or a Synchrotron facility. IR spectra were measured using Nicolet 6700 spectrometer. Synthesis and characterization procedures, experimental methods, and details of the computational approach are in the Supporting Information.

Received: June 19, 2012

Published online: August 7, 2012

Keywords: infrared spectroscopy · metal–organic framework · modeling studies · stability · zirconium

- [1] a) G. Férey, *Chem. Soc. Rev.* **2008**, 37, 191; b) O. M. Yaghi, M. O’Keeffe, N. W. Ockwig, H. K. Chae, M. Eddaoudi, J. Kim, *Nature* **2003**, 423, 705; c) S. Kitagawa, S. Noro, *Angew. Chem.* **2004**, 116, 2388; *Angew. Chem. Int. Ed.* **2004**, 43, 2334.
- [2] Themed issue: Metal–Organic Frameworks, *Chem. Soc. Rev.* **2009**, 38, 1201; *Chem. Rev.* **2012**.
- [3] a) M. Dineia, J. R. Long, *Angew. Chem.* **2008**, 120, 6870; *Angew. Chem. Int. Ed.* **2008**, 47, 6766; b) G. Férey, C. Serre, T. Devic, G. Maurin, H. Jobic, P. L. Llewellyn, G. De Weireld, A. Vimont, M. Daturi, J.-S. Chang, *Chem. Soc. Rev.* **2011**, 40, 550.
- [4] A. Corma, H. Garcia, F. X. Llabrés i Xamena, *Chem. Rev.* **2010**, 110, 4606.
- [5] a) P. Horcajada, R. Gref, T. Baati, P. K. Allan, G. Maurin, P. Couvreur, G. Férey, R. E. Morris, C. Serre, *Chem. Rev.* **2012**, 112, 1232.
- [6] a) J. J. Low, A. I. Benin, P. Jakubczak, J. F. Abrahamian, S. A. Faheem, R. R. Willis, *J. Am. Chem. Soc.* **2009**, 131, 15834; b) K. A. Cychoz, A. J. Matzger, *Langmuir* **2010**, 26, 17198.
- [7] C. Gomes Silva, I. Luz, F. X. Llabrés i Xamena, A. Corma, H. Garcia, *Chem. Eur. J.* **2010**, 16, 11133.
- [8] C. Serre, J. A. Groves, P. Lightfoot, A. M. Z. Slawin, P. A. Wright, N. Stock, T. Bein, M. Haouas, F. Taulelle, G. Férey, *Chem. Mater.* **2006**, 18, 1451.
- [9] J. H. Cavka, S. Jakobsen, U. Olsbye, N. Guillou, C. Lamberti, S. Bordiga, K. P. Lillerud, *J. Am. Chem. Soc.* **2008**, 130, 13850.
- [10] M. Dan-Hardi, C. Serre, T. Frot, L. Rozes, G. Maurin, C. Sanchez, G. Férey, *J. Am. Chem. Soc.* **2009**, 131, 10857.

- [11] A. D. Wiersum, E. Soubeyrand-Lenoir, Q. Yang, B. Moulin, V. Guillermin, M. B. Yahia, S. Bourrelly, A. Vimont, S. Miller, C. Vagner, M. Daturi, G. Clet, C. Serre, G. Maurin, P. L. Llewellyn, *Chem. Asian J.* **2011**, *6*, 3270.
- [12] a) L. Valenzano, B. Civalieri, S. Chavan, S. Bordiga, M. H. Nilsen, S. Jakobsen, K. P. Lillerud, C. Lamberti, *Chem. Mater.* **2011**, *23*, 1700; b) A. Schaate, S. Dühnen, G. Platz, S. Lilienthal, A. M. Schneider, P. Behrens, *Eur. J. Inorg. Chem.* **2012**, 790; c) M. Kim, S. M. Cohen, *CrystEngComm* **2012**, *14*, 4096.
- [13] A. Schaate, P. Roy, T. Preuße, S. J. Lohmeier, A. Godt, P. Behrens, *Chem. Eur. J.* **2011**, *17*, 9320.
- [14] V. Guillermin, S. Gross, C. Serre, T. Devic, M. Bauer, G. Férey, *Chem. Commun.* **2010**, 46, 767.
- [15] D. K. Smith, H. W. Newkirk, *Acta Crystallogr.* **1965**, *18*, 983.
- [16] B. Moraru, G. Kickelbick, U. Schubert, *Eur. J. Inorg. Chem.* **2001**, 1295.
- [17] a) I. A. Baburin, V. A. Blatov, L. Carlucci, G. Ciani, D. M. Proserpio, *J. Solid State Chem.* **2005**, *178*, 2452; b) <http://www.topos.ssu.samara.ru/starting.html>.
- [18] <http://som.web.cmu.edu/structures/S018-beta-Sn.html>.
- [19] F. A. Almeida Paz, Y. Z. Khimyak, A. D. Bond, J. Rocha, J. Klinowski, *Eur. J. Inorg. Chem.* **2002**, 2823.
- [20] a) M. Sanselme, J. M. Grenèche, M. Riou-Cavellec, G. Férey, *Chem. Commun.* **2002**, 2172; b) C. Volkringer, T. Loiseau, M. Haouas, F. Taulelle, D. Popov, M. Burghammer, C. Riekel, C. Zlotea, F. Cuevas, M. Latroche, D. Phanon, C. Knofelv, P. L. Llewellyn, G. Férey, *Chem. Mater.* **2009**, *21*, 5783.
- [21] S. R. Miller, P. A. Wright, C. Serre, T. Loiseau, J. Marrot, G. Férey, *Chem. Commun.* **2005**, 3850.
- [22] K. Barthelet, J. Marrot, D. Riou, G. Férey, *Angew. Chem.* **2002**, *114*, 291; *Angew. Chem. Int. Ed.* **2002**, *41*, 281.
- [23] S. Chavan, J. G. Vitillo, D. Gianolio, O. Zavorotynska, B. Civalieri, S. Jakobsen, M. H. Nilsen, L. Valenzano, C. Lamberti, K. P. Lillerud, S. Bordiga, *Phys. Chem. Chem. Phys.* **2012**, *14*, 1614.
- [24] F. Vermoortele, M. Vandichel, B. Van de Voorde, R. Ameloot, M. Waroquier, V. Van Speybroeck, D. E. De Vos, *Angew. Chem.* **2012**, *124*, 4971; *Angew. Chem. Int. Ed.* **2012**, *51*, 4887.
- [25] T. Devic, V. Wagner, N. Guillo, A. Vimont, M. Haouas, M. Pascolini, C. Serre, J. Marrot, M. Daturi, F. Taulelle, G. Férey, *Microporous Mesoporous Mater.* **2011**, *140*, 25.
- [26] A. Ö. Yazaydin, R. W. Thompson, *Microporous Mesoporous Mater.* **2009**, *123*, 169.
- [27] T. Düren, F. Millange, G. Férey, K. S. Walton, R. Q. Snurr, *J. Phys. Chem. C* **2007**, *111*, 15350.
- [28] L. D. Gelb, K. E. Gubbins, *Langmuir* **1999**, *15*, 305.
- [29] Y. S. Bae, A. Ö. Yazaydin, R. Q. Snurr, *Langmuir* **2010**, *26*, 5475.
- [30] A. J. Hernández-Maldonado, R. T. Yang, *AIChE J.* **2004**, *50*, 791.
- [31] K. W. Chapman, G. J. Halder, P. J. Chupas, *J. Am. Chem. Soc.* **2009**, *131*, 17546.
- [32] M. Kim, S. J. Garibay, S. M. Cohen, *Inorg. Chem.* **2011**, *50*, 729.
- [33] J. C. Tan, A. K. Cheetham, *Chem. Soc. Rev.* **2011**, *40*, 1059.
- [34] a) J. C. Tan, T. D. Bennett, A. K. Cheetham, *Proc. Natl. Acad. Sci. USA* **2010**, *107*, 9938; b) T. Wu, J. Zhang, C. Zhou, L. Wang, X. Bu, P. Feng, *J. Am. Chem. Soc.* **2009**, *131*, 6111; c) J. Zhang, T. Wu, C. Zhou, S. Chen, P. Feng, X. Bu, *Angew. Chem.* **2009**, *121*, 2580; *Angew. Chem. Int. Ed.* **2009**, *48*, 2542.
- [35] V. Barone, M. Casarin, D. Forrer, M. Pavone, M. Sambì, A. Vittadini, *J. Comput. Chem.* **2009**, *30*, 934.